Linking Atmospheric Cloud Radiative Effects, Tropical Precipitation, and Column Relative Humidity

Michael R. Needham[1], **David A. Randall**[1]

[1]Department of Atmospheric Science, Colorado State University, Fort Collins, CO, USA

Key Points:

- The atmospheric cloud radiative effect (ACRE) depends on the column relative humidity (CRH) in a way similar to precipitation
- The CRH can be used to estimate ACRE on annual, monthly, and daily time scales in the tropics
- Longwave cloud feedback suggested to explain the documented relationship between CRH and precipitation

Corresponding author: Michael R. Needham, `m.needham@colostate.edu`

Abstract

Work in recent decades has demonstrated a robust relationship between tropical precipitation and the column relative humidity (CRH). This study identifies a similar relationship between CRH and the atmospheric cloud radiative effect (ACRE) calculated from satellite observations. Like precipitation, the ACRE begins to increase rapidly when the CRH exceeds a critical value near 75%. We show that the tight relationship between CRH and ACRE allows the ACRE to be estimated from the CRH calculated from reanalysis fields, similar to the way that CRH has been used to estimate precipitation. Our method reproduces the annual mean spatial structure of ACRE in the tropics, and skillfully estimates the mean ACRE on monthly and daily timescales in six regions of the tropics. We speculate that this link between ACRE and CRH is important to longwave cloud feedbacks which have recently been identified as important to many processes.

Plain Language Summary

The tropical precipitation rate can be estimated using a quantity called the column relative humidity (CRH), which describes how close the atmosphere is to becoming saturated with water. We show that the CRH can also be used to estimate the local radiative heating of the atmosphere due to clouds. Our simple method can reproduce the average cloud radiative heating of the tropical atmosphere, and can be used to estimate the monthly averaged and daily averaged heating in several different tropical regions. Understanding the relationship between clouds and radiative heating has recently been identified as important to processes such as the formation of hurricanes and periods of alternating enhanced and suppressed precipitation near southeast Asia.

1 Introduction

The effects of clouds on the Earth's radiation balance can be quantified using the cloud radiative effect (CRE), defined as the difference between full-sky and clear-sky radiative fluxes (Ramanathan, 1987). The CRE manifests at the top of the atmosphere, where clouds increase the reflection of solar radiation while they simultaneously enhance greenhouse warming; at the surface, where cloud shading prevents solar absorption at the ground at the same time as clouds emit infrared radiation downwards; or in the atmosphere itself, where clouds warm or cool locally by absorbing or emitting radiation.

A large body of work has investigated the impact of this atmospheric cloud radiative effect (ACRE) on the Earth's global circulation patterns (Slingo & Slingo, 1988; Randall et al., 1989; Sherwood et al., 1994; Stevens et al., 2012; Li et al., 2015; Voigt & Albern, 2019). For example, the ACRE has been found to widen the subsiding branches of the Hadley cells and to narrow the ITCZ and its associated precipitation maximum (Harrop & Hartmann, 2016; Popp & Silvers, 2017; Albern et al., 2018; Dixit et al., 2018).

Relevant to this study, the longwave cloud heating has been identified as an important feedback mechanism in the context of, for example, the initial development of tropical cyclones, the persistence of convective self-aggregation, as well as the Madden–Julian oscillation (Bretherton et al., 2005; Arnold & Randall, 2015; Wing et al., 2017; Khairoutdinov & Emanuel, 2018; Emanuel, 2019; Ruppert et al., 2020). The longwave ACRE can be a strong localized atmospheric heating which induces a thermally direct circulation connecting humid and dry regions. This circulation transports moisture against the gradient into humid regions, allowing for increased precipitation and cloudiness.

Our goal in this study is to link this longwave cloud feedback to the observed relationship between tropical precipitation and the column relative humidity (CRH, known alternatively as the saturation fraction), defined as the ratio between the water vapor path and saturation water vapor path. Observational and modeling studies in recent decades have shown a strong link between atmospheric humidity and tropical precipitation (Zeng, 1999; Raymond, 2000; Bretherton et al., 2004; Raymond & Zeng, 2005; Raymond et al., 2009; Rushley et al., 2018; Powell, 2019; Wolding et al., 2020). Bretherton et al. (2004) demonstrated that the mean precipitation rate derived from satellite observations was a strong function of the CRH. They showed that tropical precipitation could be modeled as an exponential function of CRH, and this relationship has been used in many applications including theoretical studies of the MJO (see Rushley et al. (2018), and references therein).

In this study we explore the relationship between CRH and ACRE and possible connections to the relationship between CRH and precipitation. Section 2 provides a description of data. In section 3, the ACRE is shown to be a strong function of the CRH, suggesting that the CRH can be used to estimate the ACRE. This possibility is explored in section 4, where the estimate is evaluated on annual mean, monthly, and daily time scales. We also suggest that the exponential relationship between CRH and tropical precipitation is a necessary consequence of the longwave cloud feedback described in previous studies. Conclusions are presented in section 5.

2 Data and Methods

Top of atmosphere and surface fluxes of longwave and shortwave radiation come from the CERES satellite SYN1deg Ed4a product (Doelling et al. (2013), hereafter CERES). CERES data were downloaded on a $1^\circ \times 1^\circ$ grid at a daily mean temporal resolution. Radiative fluxes were used to calculate the CRE as the difference between full-sky and clear-sky fluxes. The CRE was evaluated at the top of atmosphere and at the surface, and the ACRE was calculated as the difference between the two.

The TRMM Multisatellite Precipitation Analysis 3B42 product (hereafter TRMM) combines passive microwave data from a variety of satellites to provide estimates of precipitation rates on a $0.25^\circ \times 0.25^\circ$ grid at 3 hour increments (Huffman et al., 2016). The TRMM data were averaged to daily means and to a coarser $1^\circ \times 1^\circ$ grid to align with the CERES data. In section 3 these data are compared to two empirical models of precipitation presented by Rushley et al. (2018). Both models use an exponential curve of the form

$$P = P_r \exp(a_d \mathrm{CRH}) \tag{1}$$

where CRH is the column relative humidity as a fraction, and P_r and a_d are coefficients determined from the Special Sensor Microwave Imager (SSM/I) passive microwave imager onboard Defense Meteorological Satellite Program satellites. Note that SSM/I data is one of several inputs to the TRMM dataset. The coefficients for the first fit ($P_r = 4.07\times10^{-5}$ mm day^{-1} and $a_d = 16.12$) were determined from SSM/I version 5, which was the same data used by Bretherton et al. (2004). The coefficients for the second fit ($P_r = 6.89\times10^{-5}$ mm day^{-1} and $a_d = 14.72$) were determined from the updated version 7 algorithm, which was used by Rushley et al. (2018). These models are henceforth referred to as “V5” and “V7”.

Lastly, ERA5 reanalysis fields (Hersbach et al., 2018, 2020) were downloaded at a temporal resolution of 6 hours on the native $0.25^\circ \times 0.25^\circ$ grid. Specific humidity and temperature were used to calculate the column relative humidity as

$$\mathrm{CRH} = \frac{\int_{p_t}^{p_s} q dp}{\int_{p_t}^{p_s} q^*(T) dp}, \tag{2}$$

where q^* is the saturation vapor pressure. Like the TRMM data, the ERA5 data were averaged to daily means on the coarser 1°×1° CERES grid.

Each of the three data sources spans the same 19-year period from January 1, 2001 through December 31, 2019. Analysis was restricted to the tropical belt ranging from 30°S to 30°N. In addition to the tropical belt, the analysis was repeated for six subset regions.which represent the Indo-Pacific warm pool, the Pacific ITCZ, the south Pacific convergence zone (hereafter SPCZ), the Pacific cold tongue, the Atlantic ITCZ, and the Atlantic cold tongue.

3 Precipitation and ACRE binned by CRH

3.1 Precipitation

The top panel of Fig. 1 shows the TRMM precipitation rate binned by the CRH for the entire tropical belt ranging from 30°S to 30°N. The mean curve was calculated by taking the area-weighted average precipitation rate for all grid cells that fell within each CRH bin of width 2% from 0% to 100%. The data cover the 19 year period of record, and the shading shows the region between the 25th and 75th percentiles. Consistent with previous studies, the precipitation rate follows an exponential curve, with a rapid increase in precipitation when the CRH exceeds 75% to 80%. The dotted and dashed lines shown in the top panel are curves representing the V5 and V7 precipitation rate models presented by Rushley et al. (2018). As expected, the mean TRMM precipitation rate in each bin more closely follows the V7 model, while the V5 model predicts a precipitation rate greater than the 75th percentile when the CRH exceeds 70% to 75%.

The utility of the exponential precipitation model is illustrated by comparing the middle and lower panels of Fig. 1. The tropical belt consists of extremely humid regions that receive a large amount of precipitation, such as the Indo-Pacific warm pool and the ITCZ. It also contains the cold tongue regions which are dry in a column-integrated sense, and receive relatively little precipitation on average. The nonlinear fit appears able to recreate the average behavior of precipitation, although as mentioned by Rushley et al.

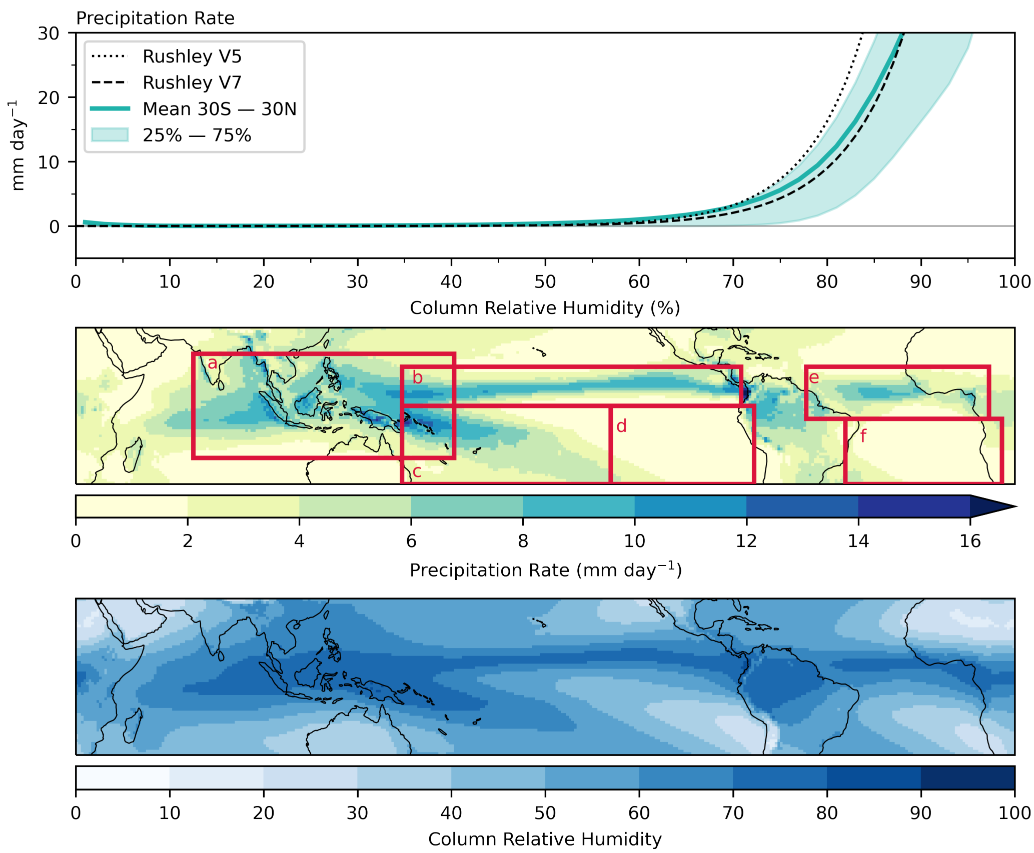

Figure 1. **Top:** 2001-2019 annual mean TRMM precipitation rate binned by column relative humidity, as well as curves showing the precipitation rate predicted by the V5 and V7 models of Rushley et al. (2018). **Middle:** Annual mean precipitation rate from TRMM. Boxes a, b, c, d, e, and f show the boundaries of the six sub-regions used throughout this study, and specific boundaries are given in Tbl. S1. **Bottom:** Annual mean column relative humidity calculated from ERA5 reanalysis.

(2018) the spread in the distribution indicates that factors other than the CRH also impact tropical precipitation.

When the binning procedure in the top panel is repeated for six regions of the tropics, the same exponential dependence of precipitation is observed (see supporting information). This occurs even though the regions are characterized by different underlying distributions of CRH. The regional precipitation rates again more closely follow the V7 model, while the V5 model tends to overestimate the precipitation rate.

3.2 ACRE

The relationship between CRH and ACRE is shown in Fig. 2. Figs. 2.a - 2.c show the longwave, shortwave, and net ACRE binned by the CRH for the entire tropical belt. The solid line shows the mean value for each CRH bin, while the shaded area again shows the region bounded by the 25th and 75th percentiles. As with the precipitation rate, each of the three curves shows a rapid increase in the magnitude of the ACRE as the CRH exceeds 70%-80%.

The shortwave ACRE is small in most regions, illustrating that solar radiation is typically transmitted through the atmosphere or reflected back to space, rather than being absorbed by clouds. The shortwave ACRE only becomes non-negligible in the most humid regions. This shows that the ACRE is largely determined by the absorption of longwave radiation, consistent with previous studies (e.g., Slingo and Slingo (1988); Allan (2011)). The longwave and shortwave effects are small and of opposite sign in dry regions but become large and positive in humid regions. The large ACRE suggests low-level convergence into humid regions (Neelin & Held, 1987), consistent with the longwave feedback described in previous studies (e.g. Ruppert et al. (2020)). Moisture convergence driven by ACRE may help to explain the increase of precipitation in regions with a large CRH.

Figs. 2.d - 2.i show the net ACRE as a function of CRH for each of the six regions. Like the wider tropical belt, the net ACRE in each of the regions is determined primarily by the longwave effect (not shown). These regional curves exhibit the same general behavior for each of the six regions, with the exception of the cold tongue regions at low CRH. Both of the cold tongue regions (panels h and i) exhibit a minimum in the ACRE near 20% representing a strong negative ACRE. This is presumably due to marine stra-

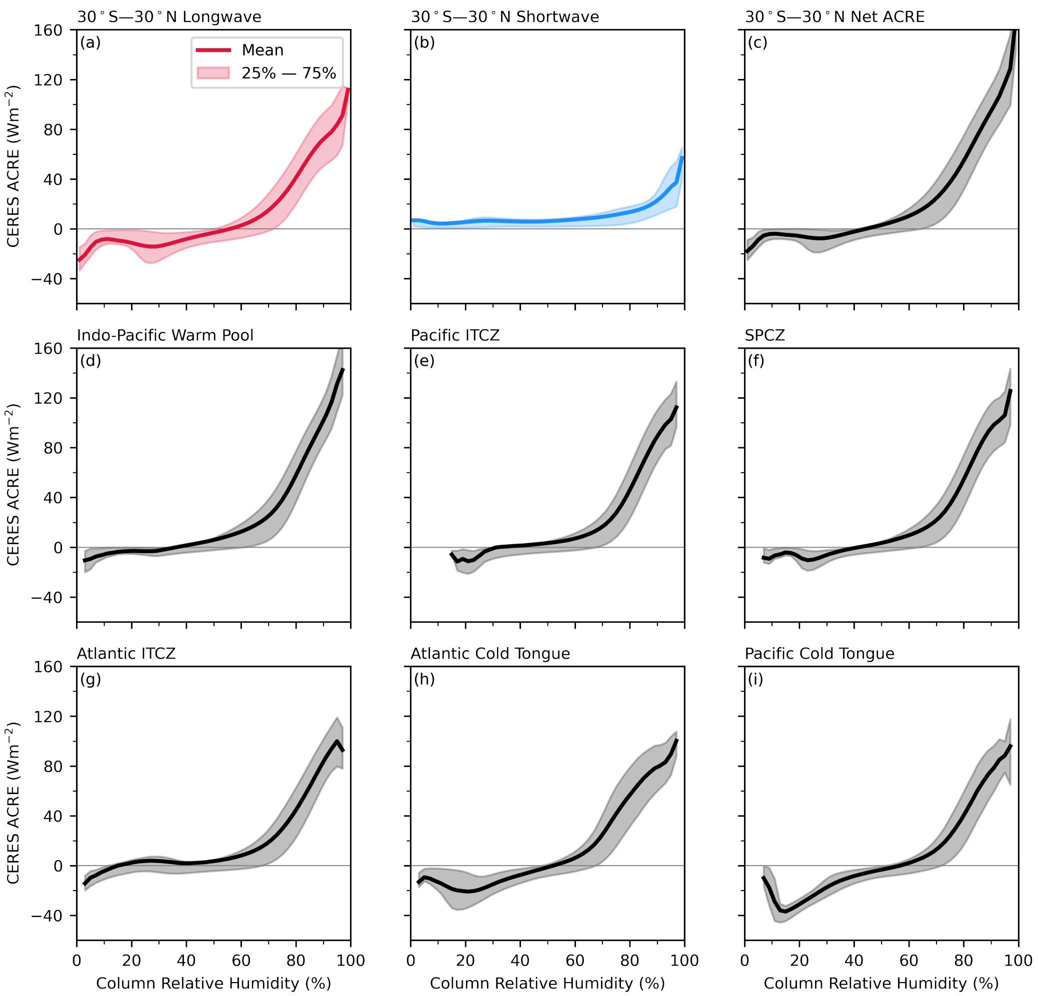

Figure 2. **(a):** Longwave ACRE binned by CRH for the belt ranging from 30°S to 30°N. The shaded area shows the region bounded by the 25th and 75th percentiles for each CRH bin. **(b):** Same as **(a)**, but for the shortwave ACRE. **(c):** Net ACRE, calculated as the sum of longwave and shortwave effects. **(d)-(i):** same as **(c)**, but for the six tropical regions defined in the text.

tus clouds which have a small greenhouse effect, but cool the atmosphere by emitting to the surface from their cloud base (Klein & Hartmann, 1993). The similarity of the curves in Fig. 2 suggests that CRH may be used to predict the ACRE, similar to the way that it is used to predict precipitation. This possibility is explored in the next section.

4 Estimating ACRE from CRH

4.1 Annual Mean Spatial Distribution

The ACRE was estimated form the CRH using Figs. 2.a and 2.b to calculate the daily mean longwave and shortwave ACRE at each grid cell as a function of the CRH. The longwave and shortwave effects were added together to give the net ACRE, and daily means were then averaged together to give the annual mean value at each grid cell.

Fig. 3.a shows the annual mean ACRE calculated from CERES observations over the 19-year record. The spatial structure shows that absorption of longwave radiation by deep convective clouds in the Indo-Pacific, SPCZ and ITCZ regions leads to a positive ACRE. In the cold-tongue regions, marine stratus clouds lead to a negative ACRE. Averaged over the 30°S to 30°N belt, the ACRE was 15.193 Wm^{-2}. The shading in Fig. 3.b shows the annual mean ACRE estimated from CRH over the same 19 year period. The estimated ACRE largely reproduces the spatial structure of the ACRE observed from CERES. The estimation shows a large positive ACRE in the Indo-Pacific, SPCZ, and ITCZ regions, and shows a negative ACRE in the stratus regions. The annual mean ACRE estimated from CRH is 15.203 Wm^{-2}, which is an error of only about 0.01 Wm^{-2} compared to the ACRE calculated from satellite observations.

As shown in Fig. 3.c, the small error in the domain averaged ACRE is due to largely offsetting positive and negative errors. The lack of shading in about half of the domain indicates that the observed and estimated ACRE are within 5 Wm^{-2} of each other. The estimation method appears to have a positive bias in the east Pacific relative to the west Pacific. This is partially due to the longwave CRE at the top of the atmosphere (not shown), and is consistent with Kubar et al. (2007) who found that the temperature of high tropical clouds was about 5 K warmer in the east Pacific compared to those in the west Pacific. In addition, the estimation method gives negative errors over land compared to mostly positive errors over oceans. Although these errors are not negligible, this is merely the first attempt at estimating the ACRE using the CRH. A method that takes into account,

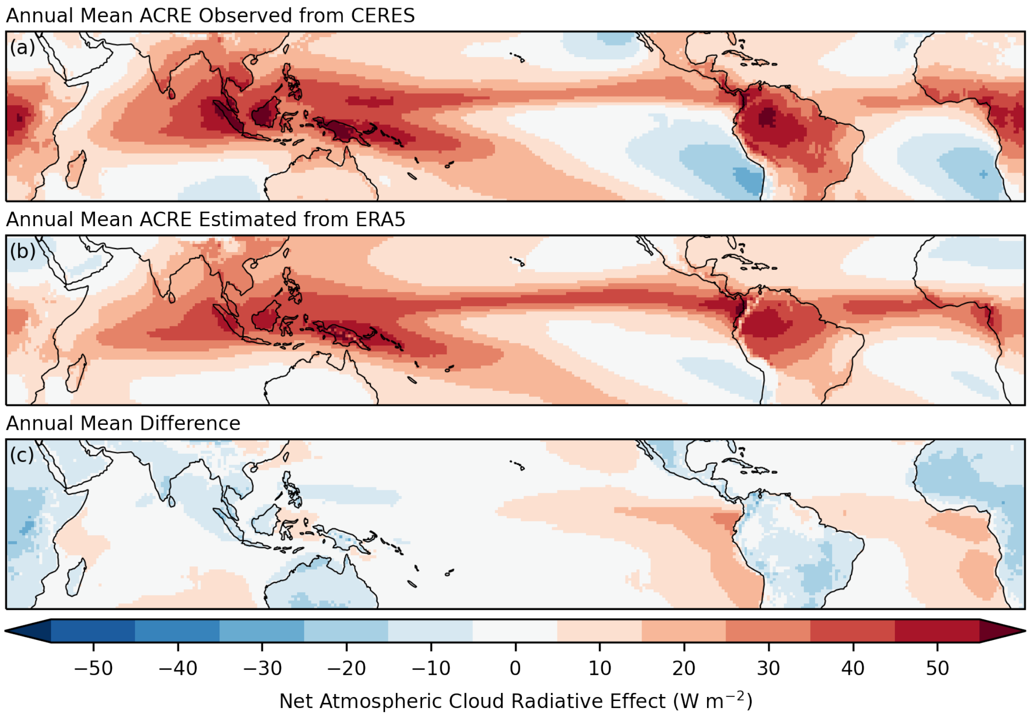

Figure 3. **(a):** Annual mean ACRE calculated from CERES radiative fluxes. **(b):** Annual mean ACRE estimated from ERA5 column relative humidity. **(c):** Difference between **(a)** and **(b)**.

for example, the total condensed liquid or ice water path to help separate low and high clouds may more accurately estimate the ACRE and help to remove regional biases. This possibility is left for future work.

4.2 Accuracy of the Estimation on Shorter Timescales

The estimation largely reproduces the annual mean spatial structure of the ACRE, but how well does it perform on shorter time scales? To answer this, Fig. 4 compares the observed and estimated monthly mean ACRE anomaly for each of the six regions. Anomalies were calculated as the average ACRE over the region minus the mean ACRE for that region for each month, effectively removing the seasonal cycle. The agreement between the observed and estimated ACRE was evaluated using Pearson's R^2 correlation, which is shown in the lower left-hand corner of each panel.

The Indo-Pacific, SPCZ, and both ITCZ regions each show a high degree of correlation, with R^2 greater than either 0.6 or 0.7. The estimation method is able to account for the large peaks in magnitude in the warm pool and pacific ITCZ regions in 2010 and 2015 to 2016 which are likely associated with the strong El Niño events of those years. The correlation is slightly lower for the cold tongue regions, with R^2 equal to 0.56 and 0.515 in the Pacific and Atlantic, respectively. Together, this indicates that more than 50% of the variance of the ACRE on monthly time scales can be explained by the CRH in each of these regions.

The R^2 correlations for the monthly mean time series are recorded in Tbl. S1, alongside the R^2 correlations for daily mean time series, which were constructed in much the same way. Unsurprisingly the agreement is lower in each region on daily time scales compared to monthly time scales, although the correlation is still greater than 0.6 in the warm pool, and greater than 0.4 in all regions except for the Pacific cold tongue. From this, it appears that the CRH method is somewhat skillful at estimating the ACRE even on time scales shorter than a month.

4.3 Discussion

What accounts for this relationship between CRH and the ACRE? Figs. 1 and 2 show that precipitation and ACRE depend on the CRH in a similar way. Both are small in magnitude when the CRH is small, and increase rapidly when the CRH exceeds a critical value between 70% to 80%. We speculate that the dependence of precipitation on CRH is linked to the ACRE in the form of the longwave cloud feedback discussed in previous studies (Bretherton et al., 2005; Arnold & Randall, 2015; Wing et al., 2017; Khairoutdinov & Emanuel, 2018; Emanuel, 2019; Ruppert et al., 2020). Briefly, clouds tend to form in humid regions, where they cause a local greenhouse effect. The convergence of energy promotes deep convection as well as large-scale ascent (Chikira, 2014; Jenney et al., 2020). The large-scale ascent moistens a deep layer of the troposphere, and drives low-level convergence (Riehl & Malkus, 1958; Neelin & Held, 1987), leading to more cloudiness and enhanced precipitation, as described by (Bretherton et al., 2004) and others.

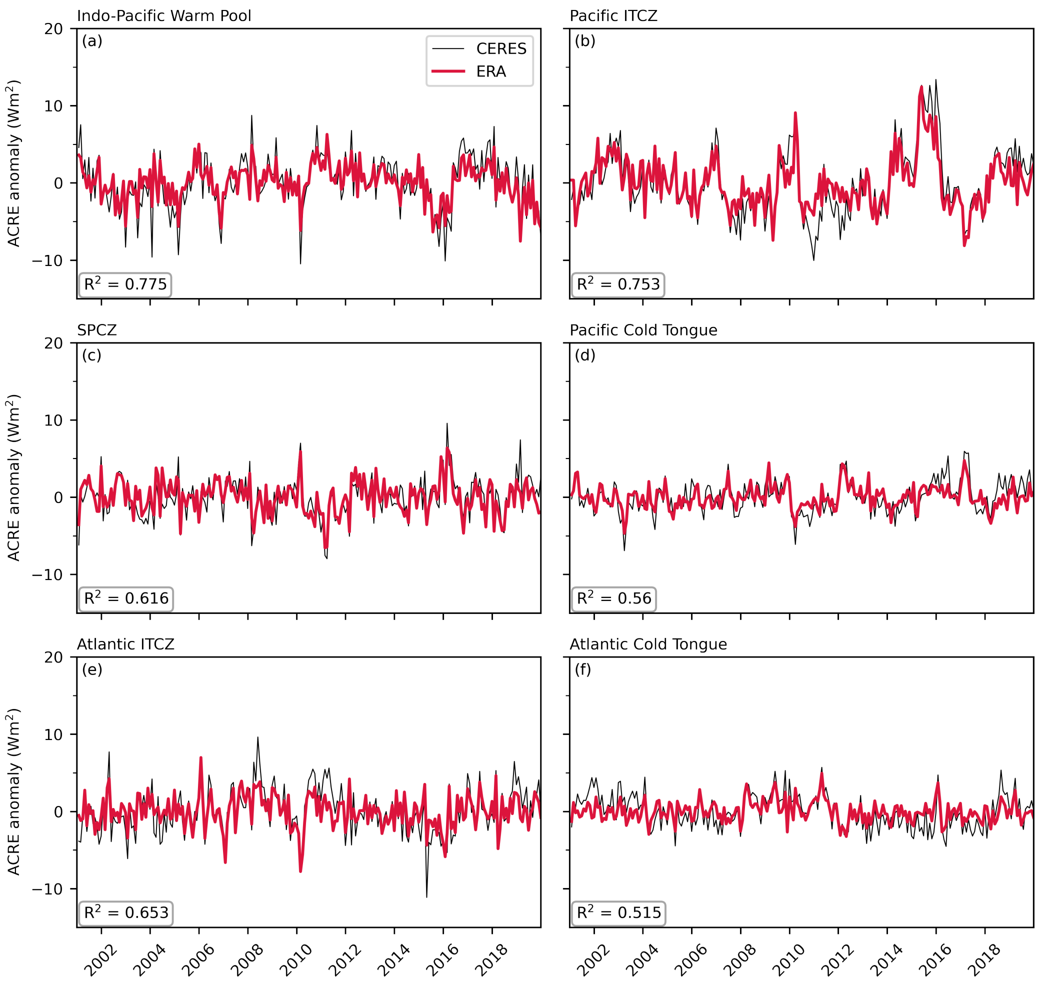

Figure 4. **(a)** De-seasonalized time series of monthly mean ACRE anomaly averaged over the Indo-Pacific warm pool. Black line shows the ACRE anomaly observed from CERES satellite fluxes, while the red line shows the ACRE anomaly estimated from ERA5. **(b)-(f):** same as **(a)**, but averaged over, respectively, the pacific ITCZ, the SPCZ, the Pacific cold tongue, the Atlantic ITCZ, and the Atlantic cold tongue. Outlines of the six regions are shown as boxes in Fig. 1.

5 Summary

We have shown that the atmospheric CRE varies with the CRH in a way that is similar to the well-documented relationship between precipitation and CRH. When the ACRE from satellite observations is binned by the CRH, the net ACRE increases rapidly as the CRH exceeds 70% to 80%. Moreover, this same behavior is seen when the calculations are repeated for six regions of the tropics with different underlying atmospheric and surface conditions.

The similarity of the curves showing the ACRE as a function of CRH in these six regions suggests that the ACRE can be estimated from the CRH, in the same way that CRH has been used to estimate precipitation. Our method was able to reproduce the large-scale annual-mean spatial distribution of ACRE in the tropics, including a well defined ITCZ and Indo-Pacific warm pool. The difference in the observed and estimated ACRE averaged over the domain is 0.01 $\mathrm{Wm^{-2}}$, due to positive and negative errors in different regions which mostly cancel. Comparisons of the observed and estimated regional time series of ACRE show a high degree of agreement on monthly time scales, with slightly less agreement on daily time scales. The method is also able to reproduce large peaks in the magnitude of the ACRE in the ITCZ and warm pool regions associated with ENSO variability. Generally the method works better in regions associated with deep convective clouds, compared to the cold tongue regions that are characterized by marine stratus clouds.

A possible explanation for the relationship between ACRE and CRH was proposed in the form of a moisture feedback driven by ACRE, which has been identified previously in a variety of contexts. The feedback suggests that atmospheric heating due to clouds leads to moisture convergence that in turn leads to the formation of more clouds as well as enhanced precipitation. This feedback will be discussed further in an upcoming paper.

Acknowledgments

All of the data used in this study are freely available online. ERA5 reanalysis data were downloaded from the ECMWF Copernicus Climate Data Store (CDS), accessible at `https://cds.climate.copernicus.eu/`. TRMM data were downloaded from the Goddard Earth Sciences Data and Information Services Center (GES DISC), accessible at `https://disc`

.gsfc.nasa.gov/. CERES SYN1deg_Ed4a data were obtained from the NASA Langley Research Center Atmospheric Science Data Center (ASDC), accessible at https://ceres.larc.nasa.gov/. This research has been partially funded by the National Science Foundation.

References

Albern, N., Voigt, A., Buehler, S. A., & Grützun, V. (2018, August). Robust and nonrobust impacts of atmospheric Cloud-Radiative interactions on the tropical circulation and its response to surface warming. *Geophys. Res. Lett.*, *27*, 4937. Retrieved from http://doi.wiley.com/10.1029/2018GL079599 doi: 10.1029/2018GL079599

Allan, R. P. (2011, September). Combining satellite data and models to estimate cloud radiative effect at the surface and in the atmosphere. *Met. Apps*, *18*(3), 324-333. doi: 10.1002/met.285

Arnold, N. P., & Randall, D. A. (2015, December). Global-scale convective aggregation: Implications for the Madden-Julian oscillation: GLOBAL-SCALE CONVECTIVE AGGREGATION. *J. Adv. Model. Earth Syst.*, *7*(4), 1499-1518. Retrieved from http://doi.wiley.com/10.1002/2015MS000498 doi: 10.1002/2015ms000498

Bretherton, C. S., Blossey, P. N., & Khairoutdinov, M. (2005, December). An Energy-Balance analysis of deep convective Self-Aggregation above uniform SST. *J. Atmos. Sci.*, *62*(12), 4273-4292. Retrieved from https://doi.org/10.1175/JAS3614.1 doi: 10.1175/JAS3614.1

Bretherton, C. S., Peters, M. E., & Back, L. E. (2004). Relationships between water vapor path and precipitation over the tropical oceans. *J. Clim.*, *17*(7), 1517-1528.

Chikira, M. (2014, February). Eastward-Propagating intraseasonal oscillation represented by Chikira–Sugiyama cumulus parameterization. part II: Understanding moisture variation under weak temperature gradient balance. *J. Atmos. Sci.*, *71*(2), 615-639. Retrieved from https://journals.ametsoc.org/jas/article/71/2/615/27839/Eastward-Propagating-Intraseasonal-Oscillation doi: 10.1175/JAS-D-13-038.1

Dixit, V., Geoffroy, O., & Sherwood, S. C. (2018, June). Control of ITCZ width by low-level radiative heating from upper-level clouds in aquaplanet simulations. *Geophys. Res. Lett.*, *45*(11), 5788-5797. Retrieved from https://onlinelibrary.wiley.com/doi/abs/10.1029/2018GL078292 doi: 10.1029/2018gl078292

Doelling, D. R., Loeb, N. G., Keyes, D. F., Nordeen, M. L., Morstad, D., Nguyen, C., ... Sun, M. (2013, June). Geostationary enhanced temporal interpolation for CERES flux products. *J. Atmos. Ocean. Technol.*, *30*(6), 1072-1090. Retrieved from https://journals.ametsoc.org/view/journals/atot/30/6/jtech-d-12-00136_1.xml doi: 10.1175/JTECH-D-12-00136.1

Emanuel, K. (2019, January). Inferences from simple models of slow, convectively coupled processes. *J. Atmos. Sci.*, *76*(1), 195-208. Retrieved from https://doi.org/10.1175/JAS-D-18-0090.1 doi: 10.1175/JAS-D-18-0090.1

Harrop, B. E., & Hartmann, D. L. (2016, April). The role of cloud radiative heating in determining the location of the ITCZ in aquaplanet simulations. *J. Clim.*, *29*(8), 2741-2763. doi: 10.1175/JCLI-D-15-0521.1

Hersbach, H., Bell, B., Berrisford, P., Biavati, G., Horányi, A., Muñoz Sabater, J., ... Thépaut, J.-N. (2018). *ERA5 hourly data on pressure levels from 1979 to present.* Retrieved from http://dx.doi.org/10.24381/cds.bd0915c6 doi: 10.24381/cds.bd0915c6

Hersbach, H., Bell, B., Berrisford, P., Hirahara, S., Horányi, A., Muñoz-Sabater, J., ... Thépaut, J. (2020, July). The ERA5 global reanalysis. *Q.J.R. Meteorol. Soc.*, *146*(730), 1999-2049. Retrieved from https://onlinelibrary.wiley.com/doi/abs/10.1002/qj.3803 doi: 10.1002/qj.3803

Huffman, G. J., Bolvin, D. T., Nelkin, E. J., & Adler, R. F. (2016). *TRMM (TMPA) precipitation L3 1 day 0.25 degree x 0.25 degree V7 (TRMM_3B42_Daily).* Retrieved from https://disc.gsfc.nasa.gov/datasets/TRMM_3B42_Daily_7/summary doi: 10.5067/TRMM/TMPA/DAY/7

Jenney, A. M., Randall, D. A., & Branson, M. D. (2020, May). Understanding the response of tropical ascent to warming using an energy balance framework. *J. Adv. Model. Earth Syst.*. Retrieved from https://onlinelibrary.wiley.com/doi/abs/10.1029/2020MS002056 doi: 10.1029/2020MS002056

Khairoutdinov, M. F., & Emanuel, K. (2018, December). Intraseasonal variability in a Cloud-Permitting Near-Global equatorial aquaplanet model. *J. Atmos. Sci.*, *75*(12), 4337-4355. Retrieved from `https://journals.ametsoc.org/view/journals/atsc/75/12/jas-d-18-0152.1.xml` doi: 10.1175/JAS-D-18-0152.1

Klein, S. A., & Hartmann, D. L. (1993, August). The seasonal cycle of low stratiform clouds. *J. Clim.*, *6*(8), 1587-1606. doi: 10.1175/1520-0442(1993)006⟨1587:TSCOLS⟩2.0.CO;2

Kubar, T. L., Hartmann, D. L., & Wood, R. (2007, November). Radiative and convective driving of tropical high clouds. *J. Clim.*, *20*(22), 5510-5526. doi: 10.1175/2007JCLI1628.1

Li, Y., Thompson, D. W. J., & Bony, S. (2015, September). The influence of atmospheric cloud radiative effects on the Large-Scale atmospheric circulation. *J. Clim.*, *28*(18), 7263-7278. Retrieved from `https://journals.ametsoc.org/view/journals/clim/28/18/jcli-d-14-00825.1.xml?tab_body=pdf` doi: 10.1175/JCLI-D-14-00825.1

Neelin, J. D., & Held, I. M. (1987). Modeling tropical convergence based on the moist static energy budget. *Mon. Weather Rev.*, *115*(1), 3–12.

Popp, M., & Silvers, L. G. (2017, November). Double and single ITCZs with and without clouds. *J. Clim.*, *30*(22), 9147-9166. doi: 10.1175/JCLI-D-17-0062.1

Powell, S. W. (2019, December). Observing possible thermodynamic controls on tropical marine rainfall in moist environments. *J. Atmos. Sci.*, *76*(12), 3737-3751. doi: 10.1175/jas-d-19-0144.1

Ramanathan, V. (1987). The role of earth radiation budget studies in climate and general circulation research. *J. Geophys. Res.*, *92*(D4), 4075. doi: 10.1029/JD092iD04p04075

Randall, D. A., Harshvardhan, Dazlich, D. A., & Corsetti, T. G. (1989, July). Interactions among radiation, convection, and Large-Scale dynamics in a general circulation model. *J. Atmos. Sci.*, *46*(13), 1943-1970. Retrieved from `https://journals.ametsoc.org/jas/article/46/13/1943/22282/Interactions-among-Radiation-Convection-and-Large` doi: 10.1175/1520-0469(1989)046⟨1943:IARCAL⟩2.0.CO;2

Raymond, D. J. (2000, July). Thermodynamic control of tropical rainfall. *Q.J.R. Meteorol. Soc.*, *126*(564), 889-898. doi: 10.1002/qj.49712656406

Raymond, D. J., Sessions, S. L., Sobel, A. H., & Fuchs, Ž. (2009, March). The mechanics of gross moist stability. *J. Adv. Model. Earth Syst.*, *1*(3). doi: 10.3894/JAMES.2009.1.9

Raymond, D. J., & Zeng, X. (2005, April). Modelling tropical atmospheric convection in the context of the weak temperature gradient approximation. *Quart. J. Roy. Meteor. Soc.*, *131*(608), 1301-1320. doi: 10.1256/qj.03.97

Riehl, H., & Malkus, J. S. (1958). On the heat balance in the equatorial trough zone. *Geophysica*, *6*, 503-537.

Ruppert, J. H., Jr, Wing, A. A., Tang, X., & Duran, E. L. (2020, November). The critical role of cloud-infrared radiation feedback in tropical cyclone development. *Proc. Natl. Acad. Sci. U. S. A.*, *117*(45), 27884-27892. Retrieved from `http://dx.doi.org/10.1073/pnas.2013584117` doi: 10.1073/pnas.2013584117

Rushley, S. S., Kim, D., Bretherton, C. S., & Ahn, M.-S. (2018, January). Reexamining the non-linear moisture-precipitation relationship over the tropical oceans. *Geophys. Res. Lett.*, *45*(2), 1133-1140. doi: 10.1002/2017GL076296

Sherwood, S. C., Ramanathan, V., Barnett, T. P., Tyree, M. K., & Roeckner, E. (1994). Response of an atmospheric general circulation model to radiative forcing of tropical clouds. *J. Geophys. Res.*, *99*(D10), 20829. doi: 10.1029/94jd01632

Slingo, A., & Slingo, J. M. (1988, July). The response of a general circulation model to cloud longwave radiative forcing. i: Introduction and initial experiments. *Q.J Royal Met. Soc.*, *114*(482), 1027-1062. doi: 10.1002/qj.49711448209

Stevens, B., Bony, S., & Webb, M. (2012, September). *CLOUDS ON-OFF KLIMATE INTERCOMPARISON EXPERIMENT (COOKIE).* `http://www.euclipse.eu/wp4/wp4.html`. Retrieved from `http://www.euclipse.eu/wp4/wp4.html` (Accessed: 2020-7-28)

Voigt, A., & Albern, N. (2019, December). No cookie for climate change. *Geophys. Res. Lett.*, *46*(24), 14751-14761. Retrieved from `https://onlinelibrary.wiley.com/doi/abs/10.1029/2019GL084987` doi: 10.1029/2019GL084987

Wing, A. A., Emanuel, K., Holloway, C. E., & Muller, C. (2017, November). Convective Self-Aggregation in numerical simulations: A review. *Surv. Geophys.*, *38*(6), 1173-1197. doi: 10.1007/s10712-017-9408-4

Wolding, B., Dias, J., Kiladis, G., Ahmed, F., Powell, S. W., Maloney, E., & Branson, M. (2020, May). Interactions between moisture and tropical convection. part i: The coevolution of moisture and convection. *J. Atmos. Sci.*, *77*(5), 1783-1799. doi: 10.1175/jas-d-19-0225.1

Zeng, X. (1999, August). The relationship among precipitation, Cloud-Top temperature, and precipitable water over the tropics. *J. Clim.*, *12*(8), 2503-2514. Retrieved from `https://journals.ametsoc.org/view/journals/clim/12/8/1520-0442_1999_012_2503_trapct_2.0.co_2.xml` doi: 10.1175/1520-0442(1999)012⟨2503:TRAPCT⟩2.0.CO;2